Published in final edited form as:
J Immunol. 2012 February 1; 188(3): 1523–1533. doi:10.4049/jimmunol.1102507.

Antiviral and regulatory T cell immunity in a patient with STIM1 deficiency[1]

Sebastian Fuchs[*,2], **Anne Rensing-Ehl**[*,2], **Carsten Speckmann**[*,†], **Bertram Bengsch**[‡], **Annette Schmitt-Graeff**[§], **Ilka Bondzio**[*], **Andrea Maul-Pavicic**[*], **Thilo Bass**[¶], **Thomas Vraetz**[*,†], **Brigitte Strahm**[†], **Tobias Ankermann**[#], **Melina Benson**[**], **Almuth Caliebe**[††], **Regina Fölster-Holst**[‡‡], **Petra Kaiser**[§§], **Robert Thimme**[‡], **Wolfgang W. Schamel**[*,¶], **Klaus Schwarz**[*,¶¶], **Stefan Feske**[**], and **Stephan Ehl**[*,†,3]

[*]Centre of Chronic Immunodeficiency, University of Freiburg, Germany

[†]Center for Pediatrics and Adolescent Medicine, University of Freiburg, Germany

[‡]Department of Medicine II, University Hospital Freiburg, Freiburg, Germany

[§]Institute of Pathology, University Medical Center, Freiburg, Germany

[¶]Faculty of Biology and BIOSS Centre for Biological Signalling Studies, University of Freiburg, Germany

[||]Max Planck Institute of Immunobiology and Epigenetics, Freiburg, Germany

[#]Department of Pediatrics, University Hospital of Schleswig-Holstein, Campus Kiel, Germany

[**]Department of Pathology, New York University, Langone Medical Center, New York, NY

[††]Institute for Human Genetics, Christian-Albrechts University and University Hospital of Schleswig-Holstein, Campus Kiel, Germany

[‡‡]Clinic for Dermatology, Venereology and Allergy, University Hospital of Schleswig-Holstein, Campus Kiel, Germany

[§§]Professor-Hess-Kinderklinik, Bremen, Germany

[¶¶]Institute of Transfusion Medicine, University of Ulm and Institute of Clinical Transfusion Medicine and Immunogenetics, Ulm, Germany

Abstract

[1]This work was supported by grants from the BMBF (BMBF 01 EO 0803; to S.E.), the Deutsche Forschungsgemeinschaft (grants SFB620 TP A4 and B6; to S.E. and W.W.S., respectively; Emmy Noether program; to T.B. and W.W.S.), and US National Institutes of Health grant AI066128 (to S. Feske).

[4]Abbreviations used in this manuscript: STIM, stromal interaction molecule; SOCE, store operated calcium entry; FOXP3, forkhead box protein 3; Treg, regulatory T cell; ER, endoplasmic reticulum; CRAC, calcium-release activated calcium.

[3]Corresponding author: Prof. Dr. Stephan Ehl, Centre of Chronic Immunodeficiency, University Hospital Freiburg, Breisacher Str. 117, 79106 Freiburg, Germany; Phone: +49(0)761/27077300, FAX: +49 (0)761/27077600, stephan.ehl@uniklinik-freiburg.de.
[2]The first two authors have contributed equally to this manuscript.

Authorship contributions

S.E. initiated the study and designed it together with S.Fuchs, A.R.-E. and R.T.. Experiments were performed and analyzed by S.Fuchs, A.R.-E., B.B., T.B. Histology and immunohistochemistry was performed by A.S.-G.. S.Feske and M.B. performed Westernblot. W.W.S., R.T. and A.M.-P. contributed to analytic tools and methods. Clinical, diagnostic and genetic workup were provided by S.E., C.S., I.B.,T.V.,B.S.,T.A., A.C., R.F.-H., P.K and K.S.. S.Fuchs, A.R.-E. and S.E. wrote the manuscript.

Conflict of interest disclosures

The authors do not have financial conflicts of interest.

Stromal interaction molecule 1 (STIM1)[4] deficiency is a rare genetic disorder of store-operated Calcium entry (SOCE), associated with a complex syndrome including immunodeficiency and immune dysregulation. The link from the molecular defect to these clinical manifestations is incompletely understood. We report 2 patients with a homozygous R429C point mutation in *STIM1* completely abolishing SOCE in T cells. Immunological analysis of one patient revealed that despite the expected defect of T cell proliferation and cytokine production *in vitro*, significant antiviral T cell populations were generated *in vivo*. These T cells proliferated in response to viral antigens and showed normal antiviral cytotoxicity. However, antiviral immunity was insufficient to prevent chronic CMV and EBV infections with a possible contribution of impaired NK cell function and a lack of NKT cells. Furthermore, autoimmune cytopenia, eczema and intermittent diarrhea suggested impaired immune regulation. Forkhead box protein 3 (FOXP3) positive regulatory T cells (Treg) were present but showed an abnormal phenotype. The suppressive function of STIM1 deficient Treg cells *in vitro*, however, was normal. Given these partial defects in cytotoxic and regulatory T cell function, impairment of other immune cell populations probably contributes more to the pathogenesis of immunodeficiency and autoimmunity in STIM1 deficiency than previously appreciated.

Introduction

Calcium signals play a key role in the activation, differentiation and effector functions of lymphocytes (1). Immunoreceptor engagement leads to a short-term increase of cytosolic Ca^{2+} by emptying endoplasmatic reticulum (ER) stores. The sustained rise in intracellular Ca^{2+} required for proliferation and effector functions then requires additional Ca^{2+} influx from the extracellular space. In lymphocytes, this is mediated by store-operated calcium entry (SOCE) through calcium-release activated calcium (CRAC) channels (2). The stromal interaction molecule STIM1 senses the decrease in Ca^{2+} concentration in the ER (3, 4) and activates ORAI1, the pore-forming subunit of the CRAC channel in the plasma membrane (5-7). The key role for STIM1 and ORAI1 in the human immune system is well illustrated by patients with defects in the genes encoding these proteins, who present with a severe form of combined immunodeficiency (8). Six patients with ORAI1 deficiency and four patients with STIM1 deficiency have so far been published (9–11) and they all shared a phenotype of severe viral, bacterial and fungal infections.

Immunological observations in these patients have helped to understand this phenotype. In patients with CRAC channel disorders, the numbers of circulating T, B and NK cells were normal or elevated (8). However, T cell activation was severely impaired, mainly due to a failure to activate NFAT (12). Thus, T cell proliferative responses to a variety of stimuli *in vitro* were reduced or absent (10, 12–14) and there was a severe defect in the production of cytokines (15). Immunoglobulin levels and specific antibodies were variable, but normal in some patients (9–12). Moreover, NK cell cytotoxicity as well as cytokine production induced by target cell recognition was severely impaired (16). While these results provide a framework for the explanation of the infection susceptibility, a number of questions remain unresolved. The spectrum of antimicrobial effector cells and effector mechanisms affected by the human CRAC channel disorders remains incompletely characterized. Moreover, the relative role of defects in T cell priming, proliferation, differentiation and effector function in the failure of antiviral defence has not been defined. In particular, virus-specific T cell responses have not been analyzed.

Another important aspect of the phenotype of human CRAC channel disorders is an impairment of immune regulation that has predominantly been observed in patients with STIM1 deficiency. All four published patients showed autoimmune cytopenia and several showed lymphoproliferation and prolonged diarrhea (10). Due to the pleiotropic function of

Ca^{2+} flux in lymphocytes, multiple checkpoints of autoimmunity are likely to be affected. In particular, a role for impaired T cell regulation has been postulated. Reduced Treg numbers have been reported in a single STIM1 deficient patient and in mice with T cell specific deletion of STIM1 and STIM2, adoptive transfer of wild-type Treg cells can suppress the lymphoproliferative phenotype (10, 17). However, a more detailed phenotypic analysis of human STIM1 deficient Treg cells has not been reported, and due to the small number of patients, the phenotypic spectrum of impaired immune regulation in STIM1 deficiency remains incomplete.

Here, we present the first detailed immunological analysis of human STIM1 deficiency in two new patients with a homozygous Arg429Cys point mutation in STIM1 leading to absent Ca^{2+} flux in T cells. Surprisingly, we found significant residual antiviral and regulatory T cell responses, suggesting that SOCE is not limiting for many aspects of these immune functions. Rather, the combination of partially impaired T cell activation and effector functions with defects in other lymphocyte populations is likely to provide the immunological basis for the clinical phenotype of immunodeficiency with immune dysregulation.

Methods

Case reports

A six year-old girl born to consanguineous Pakistani parents (P5) initially presented with autoimmune hemolytic anemia and thrombocytopenia at the age of 10 weeks (Fig. 1A). She had recurrent bacterial and viral pneumonias, recurrent HSV stomatitis and was diagnosed with chronic EBV and CMV viraemia at the age of 4 years. She has generalized eczema since her first year of life (Fig. 1B), and developed intermittent joint effusions in her fourth year of life (ANA titer 1:5120). She further suffers from moderate colitis with recurrent episodes of diarrhea since the age of five. Colonoscopy showed mild unspecific eosinophilic inflammation and an increase in lymphatic tissue. Further clinical findings included an anhydrosis despite histologically proven presence of sweat glands, an enamel defect of her teeth (Fig. 1C), nail dysplasia (Fig. 1D), mild muscular hypotonia, light-insensitive pupils and primary enuresis. A younger sister (P6) had died at the age of 21 months due to suspected sepsis after an almost identical history including early-onset autoimmune cytopenia, recurrent pneumonias, chronic EBV and CMV viraemia and recurrent HSV infections. Both patients had T lymphocytosis, P5 had diminished, P6 normal NK and B cell numbers (Fig. 1A). Immunoglobulin levels including IgE were normal. Specific antibodies were detectable against tetanus, rubella, EBV, CMV and HSV, but not against *Haemophilus influenza B*, *pneumococcae*, measles and mumps. After the molecular diagnosis had been established, P5 received a cord blood stem cell graft following conditioning with treosulfane and fludarabine. Unfortunately she rejected the graft and currently she is well under supportive treatment while waiting for a second transplant. Informed consent for the performed studies was obtained from the patient's family in accordance with the Declaration of Helsinki and Institutional Review Board approval from the University of Freiburg Ethics Committee.

Genomic sequencing and Western Blotting

Genomic DNA was used for exon PCR amplification and capillary sequencing (primer sequences available on request). Immunoblotting was done as described with standard protocols using an affinity purified rabbit polyclonal anti-STIM1 antibody (10).

Cells

PBMC were isolated by Percoll density gradient centrifugation (Pan Biotech). Total $CD3^+$ T cells, $CD4^+CD25^+$ Treg cells and $CD3^-CD56^+$ NK cells were isolated using MACS technology (Miltenyi Biotec). T cell blasts were generated by stimulation of PBMC with Phytohemagglutine (PHA; Remel; 1,25 μg/ml) and IL-2 (Novartis; 100 U/ml) for 5–7 days. Virus specific T cells were expanded using CMV peptide pp65 495-504 (Proimmune; 10 ng/ml) and anti-CD28 antibody (BD; 0,5 μg/ml) in IMDM with 10% human AB serum and IL-2 (20 U/ml). The human erythroleukemia cell line K562 and the mouse leukemia cell line L1210 (all from ATCC, Manassas, USA) were used as target cells in cytotoxicity assays.

Antibodies for flow cytometry

The antibodies used for lymphocyte phenotyping, Vβ repertoire analysis and intracellular FACS staining are listed in supplementary Table 1. B cell subsets were stained as described (18). Tetramer staining of virus specific T cells was performed as described (19). Data acquisition was performed with the Gallios flow cytometer (Beckmann-Coulter), FACS Canto or LSRII (BD). Data were analyzed using FlowJo v 7.2.5 analysis software.

Calcium flux

MACS isolated T cells were labelled with Indo-1 AM (Invitrogen; 5 μg/ml). Some of the cells were preincubated with anti-CD3 antibody (clone OKT3, custom-made; 5 μg/ml). The cells were adjusted to a concentration of $1x10^6$ per ml in Ca^{2+}-free PBS and 1% FCS. To induce store-depletion, T cells were stimulated with Thapsigargin (1μM). Cells preincubated with anti-CD3 were stimulated with anti-Fc $F(ab')_2$ fragment (AffiniPure F(ab')2 Fragment Goat Anti-mouse IgG, Jackson ImmunoResearch; 12 ng/ml). $CaCl_2$ was then added to the cells in a final concentration of 2 mM. The measurement was performed using an LSR II flow cytometer (BD) and analysed with FlowJo software version 7.2.5.

Degranulation and cytotoxicity assays

Degranulation and cytotoxicity assays with unstimulated or IL-2 activated NK cells were performed as described (16). For analysis of anti-CD3 mediated redirected lysis, PHA/IL-2 T cell blasts were cocultured for 4,5h with ^{51}Cr labelled L1210 target cells, preincubated with anti-CD3. For antigen specific lysis, autologous EBV blasts were labelled with ^{51}Cr and loaded with CMV peptide pp65 495-504 (Proimmune; 10 ng/ml) or left unlabelled. These cells were co-cultured for 4,5h with expanded antigen specific T cell blasts. ^{51}Cr release was measured in the supernatant with scintillator plates on a Topcount luminometer (Perkin Elmer) and the percentage of specific lysis was calculated.

Early T cell activation and proliferation

$2x10^5$ PBMC were incubated for 4h with PMA (Sigma; 50 ng/ml) and Ionomycin (Sigma; 1 μg/ml) or for 16h with anti-CD3/CD28 beads (Invitrogen; 2 beads per cell). Cells were stained with anti-CD25 and CD69 antibodies before and after stimulation and analyzed by flow cytometry. For proliferation analysis, PBMC were labelled with CFSE (0,5 μM; Invitrogen) for 15 min at 37°C. Cells were stimulated with anti-CD3/CD28 beads (2 beads/cell; Invitrogen) or PHA (2,5 μg/ml; Remel) for 4–6 days. Proliferation of EBV specific T cells was assessed by coculture of $2x10^5$ CFSE labelled PBMC and $4x10^4$ irradiated (30 Gy) autologous EBV LCL with IL-2 (40 U/ml) for 5 days.

Treg suppression assay

PBMC of the patient and healthy controls were separated into $CD4^+CD25^-$ responder cells and $CD4^+CD25^+$ Treg cells by MACS (Regulatory $CD4^+CD25^+$ T cell isolation kit, Miltenyi Biotec). Responder cells were labelled with CFSE (Molecular probes; 0,5 μM).

$5x10^4$ T responder cells and $5x10^4$ ($2,5x10^4$, $1,25x10^4$) Treg cells were co-cultured for four days in IMDM+10% human AB serum (Lonza), stimulated with $2x10^5$ irradiated allogeneic PBMC and 1 μg/ml anti-CD3 (clone Hit3a).

Cytokine expression of T and NK cells

For T cell cytokine induction $1x10^6$ PBMC were stimulated with either PMA (50 ng/ml; Sigma) and Ionomycin (1 μg/ml; Sigma) for 4h or with anti-CD3/CD28 beads (Invitrogen; 2 beads per cell) for 16h in the presence of Brefeldin A (Golgiplug 1:1000; BD). Cells were surface stained, fixed/permeabilized (Cytofix/Cytoperm plus Kit, BD) and stained with the respective anti-cytokine antibodies. For determination of cytokine production by NK cells, either $5x10^5$ PBMC were coincubated with $2x10^5$ K562 target cells for 5h or $5x10^5$ MACS purified NK cells were stimulated with IL-12 (10 ng/ml; R&D systems) and IL-15 (30 ng/ml; Peprotech) for 16 hours. Brefeldin A was added for the last 4h. Cells were surface stained with anti-CD3 and anti-CD56 and with the respective anti-cytokine antibodies as described for T cells.

Immunohistochemistry

Biopsies from the left lower lobe of the lung and hilar lymph nodes were fixed in 4% buffered formaldehyde. Three- μm-thick sections were deparaffinized in xylene, rehydrated through graded alcohols subjected to antigen retrieval in a pressure cooker using a retrieval buffer (DAKO). Immunodetection was performed using the LSAB visualization system in an Austostainer plus (DAKO). The primary antibodies used are listed in supplementary table 1. All sections were counterstained with Meyer's haemalaun. Negative controls were obtained by omitting the primary antibody. Chromogen-based in situ hybridization (CISH) for the detection of Epstain-Barr virus encoded RNAs (EBER1,-2) was performed using a biotin-labelled probe (ZytoFast EBV ISH, Biotin, No T-1014-400, Zytomedsystems). Denaturation and hybridization steps were carried out in a slide processing system (StatSpin ThermoBrite, Abbott Molecular). To assess the immunophenotype of EBER positive cells, CISH was combined with immunolabelling for CD20 or CD3 using the DAKO REAL Detection System (no K5005, DAKO).

Results

A novel homozygous point mutation in STIM1 causing absence of store operated Ca^{2+} influx in T cells

Since the clinical and immunological phenotype of the 2 siblings resembled that of 4 previously reported patients with STIM1 deficiency, we sequenced *STIM1* and identified in both patients a homozygous C>T exchange at cDNA position 1285 in exon 10 leading to substitution of an arginine by a cysteine at position 429. Western Blot analysis revealed that the mutated $STIM1^{Arg429Cys}$ protein was still expressed in LCL EBV blasts of P5 (Fig. 1G). Nevertheless, TCR mediated calcium influx was completely abolished in T cells from P5 (Fig. 1E). Also the depletion of ER calcium stores by thapsigargin (TG) failed to induce calcium influx in T cells (Fig. 1F). Both parents were heterozygous for the mutation (data not shown) and cells from the mother showed reduced calcium influx after TG mediated store depletion (Fig. 1F).

Destructive EBV positive lymphoproliferative disease in lung and lymph node

At the time of referral, the patient had been treated for a lung abscess following lobar pneumonia with bronchopleural fistulas developing after thoracoscopic debridement (Fig. 2A,B). Cervical lymphadenopathy and splenomegaly was noted. Histological analysis of a resected lymph node revealed that lymphoid follicles were present, but beset with massively

expanded lymphocytes, which were distributed throughout the parenchyma and the follicles (Fig. 2C-E). The reticular meshwork was partially destroyed by the lymphocyte infiltrations, which predominantly consisted of $CD3^+$ T cells accompanied by some $CD20^+$ B cells (Fig. 2F,G). Focal accumulations of $EBER^+$ lymphocytes were identified as B cell blasts, but $EBER^+$ T cells were also found (Fig. 2H and data not shown). The resected lung tissue showed similar destructive infiltrations with activated, terminally differentiated PD-1 and Granzyme B positive $CD8^+$ T cells, rarely seen in other lymphoproliferative diseases including EBV driven lymphomatoid granulomatosis (Fig. 2 J-O). This aggressive pulmonary and lymphoid EBV positive lymphoproliferative disease was successfully treated with rituximab, which led to complete virus elimination from the blood and significant regress of the lymphadenopathy.

Polyclonal T cell repertoire dominated by terminally differentiated $CD8^+$ T cells with an "exhausted" phenotype

Analysis of the T cell compartment in P5 revealed that most of the analyzed TCR Vβ-chains were expressed in normal frequencies on $CD4^+$ T cells, while there was some alteration in the Vβ repertoire of $CD8^+$ T cells, probably related to the active EBV infection (Fig. 3A). Overall, the elevated T cell numbers with a polyclonal repertoire suggested normal T cell development. The differentiation state of $CD8^+$ T cells was analyzed using the markers CD27, CCR7 and CD45RA, which allow classification of $CD8^+$ T cells from naive to terminally differentiated CTL into five subgroups (20). P5 had very few naive $CD8^+$ T cells while the proportion of terminally differentiated $CD8^+$ T cells was increased compared to healthy donors (Fig. 3B). Moreover, inhibitory receptors associated with T cell exhaustion were strongly (2B4 and PD-1) or moderately (Tim3) expressed on patient's $CD8^+$ T cells but not on CTL of the healthy control, while the expression of KLRG1 on $CD8^+$ T cells was comparable between patient and control (Fig. 3C). The accumulation of terminally differentiated $CD8^+$ T cells was not due to impaired CD95 mediated ((10) and data not shown) or anti-CD3 induced activation induced cell death (data not shown). Thus, the $CD8^+$ T cell compartment was highly activated, but high levels of "exhaustion" markers suggested poor functionality in the context of the viral infection.

STIM1 deficiency impairs T cell proliferation and cytokine production

Since STIM1 is important for TCR mediated, Ca^{2+}-dependent T cell activation, the predominance of a highly activated, terminally differentiated $CD8^+$ T cell population was not expected. We therefore analyzed T cell activation in more detail. Upregulation of CD69 after stimulation with anti-CD3/CD28 coated beads was normal, while the expression of CD25 on resting $CD4^+$ T cells and activated $CD4^+$ and $CD8^+$ T cells was lower than in T cells from a healthy control (Fig. 4A,B). Analysis of T cell proliferation by CFSE dilution revealed a severe defect in the proliferative response of STIM1 deficient $CD4^+$ T cells following stimulation with PHA or anti-CD3, whereas the proliferation of $CD8^+$ T cells was partially impaired. Addition of IL-2 was able to partially restore the proliferation of both $CD4^+$ and $CD8^+$ T cells (Fig. 4C). To analyze T cell effector functions, we determined cytokine production and cytotoxicity. After stimulation with PMA/Ionomycin, the percentage of IFN-γ producing $CD4^+$ cells was markedly reduced, while the percentage of IL-4 producing cells was within the normal range (Fig. 4D). T cells with IL-17 production were nearly absent (Fig. 4E). As expected (17), the expression of IL-2 upon T cell activation was highly deficient in STIM1 deficient $CD4^+$ T cells (Fig. 4F). In contrast to the reduced cytokine production, T cell cytotoxicity measured by anti-CD3 redirected lysis of L1210 target cells was normal (Fig. 4G). These data indicated a partial deficiency in T cell activation and effector functions.

STIM1 deficiency allows the generation of virus-specific T cell responses

To address the question whether these defects still allowed the generation of antiviral T cell responses, we quantified CMV and EBV-specific T cells isolated from P5 by tetramer staining *ex vivo*. Interestingly, we could demonstrate a significant population of CMV-specific $CD8^+$ T cells (Fig. 5A), indicating that antiviral T cells can be primed and proliferate in human STIM1 deficiency. Healthy CMV seroconverted donors show values between <1% and 30% of epitope specific CD8 T cells, with high percentages observed in elderly patients (21). Despite the highly active EBV infection, there were only few EBV LMP-2 and BMLF-1 specific $CD8^+$ T cells (Fig. 5A). However, LMP2-specific cells could be amplified after peptide stimulation *in vitro* (Fig. 5B). To further explore this issue, we stimulated CFSE labeled PBMC isolated from P5 with autologous EBV-LCL, which induced cell division in both $CD4^+$ and $CD8^+$ T cells (Fig. 5C). Also CMV-specific CTL could be amplified by peptide stimulation *in vitro* (Fig. 5D, insert). When these cells were tested for their lytic activity on autologous EBV-LCL loaded with CMV specific antigen, significant viral epitope specific target cell lysis could be observed (Fig. 5D). In contrast, epitope-specific IFN-γ production was significantly reduced (data not shown). Thus, STIM1 deficiency allowed the generation of antiviral T cells, which showed impaired cytokine production, but normal virus-specific cytotoxicity *in vitro*.

Impaired NK cell function and lack of NKT cells in STIM1 deficiency

NK cells and NKT cells can also be relevant for the control of viral infections (22, 23) and we have previously demonstrated defects in degranulation and cytotoxicity of human ORAI1 or STIM1 deficient NK cells (16). In extension of these findings, we found that impaired NK cell degranulation as assessed by expression of CD107a after stimulation with NK sensitive K562 cells could only partly be restored by IL-2 prestimulation (Fig. 6A,B). NK cytotoxicity was severely reduced in the absence of STIM1 (Fig. 6C). Similar to ORAI1 deficient NK cells (16), NK cells from P5 with a mutation in STIM1 showed poor production of IFN-γ and partially impaired production of MIP-1β after stimulation with K562 cells, while this response was normal after stimulation with IL-12 and IL-15 (Fig. 6D). Thus, the specific impairment of target cell induced degranulation and cytokine production with preservation of activation pathways mediated by cytokine receptors is comparable in ORAI1 and STIM1 deficient NK cells. Interestingly, there was a complete absence of circulating $V\alpha24^+V\beta11^+$ NKT cells in the STIM1 deficient patient. In contrast, the numbers of NKT cells in peripheral blood of both heterozygous parents were unusually high (0.56% and 0.61% of $CD3^+$ T cells for the father and the mother, respectively) compared with NKT cell counts in healthy controls with a median of 0.045% and a range of 0.008% to 0.76% in healthy donors (Fig. 6E and data not shown).

Abnormal phenotype, but normal suppressive function of STIM1 deficient regulatory T cells

One possible explanation for the autoimmunity observed in the STIM1 deficient patients is the absence of $FOXP3^+$ Treg cells as has been described in one STIM1 deficient patient (10). In P5 the frequency of $CD25^+FOXP3^+$ Treg cells was 2,5% of all $CD4^+$ T cells and therefore at the lower end of the normal range (Fig. 7A). We also observed an unusual population of $CD25^-CD4^+$ T cells expressing FOXP3. $FOXP3^+$ T cells were also found in the pulmonary lymphoproliferative lesions (Fig. 7B). Expression of CD39 has been described to correlate with the suppressive activity of the Treg cells (24). Whereas 70% of $CD25^+FOXP3^+$ Treg cells from healthy controls expressed CD39, only 30% of $CD25^+FOXP3^+$ and 8% of $CD25^-FOXP3^+$ Treg cells from the patient were positive for CD39 (Fig. 7D). Nearly all $CD4^+CD25^+$ T cells of the patient were $CD45RA^-$ and $CD45RO^+$ and most cells were CD127 negative, indicating a high activation status of the patient Treg cells (Fig. 7C). To analyze Treg function *in vitro*, we labeled allogeneic

$CD4^+CD25^-$ responder cells from a healthy donor with CFSE and stimulated these cells with irradiated allogeneic PBMC and anti-CD3 antibody. Treg cells from either the same donor or from the patient were then added to the culture and CFSE dilution was measured 3 days later (Fig. 7E and F). The $CD25^+$ Treg cells from the patient showed a suppressive activity similar to control cells. The patient Treg also suppressed autologous responder T cells, but due to their intrinsic proliferation defect, overall proliferation was lower than in control responders (data not shown). These findings suggest that the suppressive function of $CD25^+$ Treg cells does not require STIM1 dependent Ca^{2+} influx. To extend these findings, we expanded $CD4^+$ $CD25^+$ patient Treg cells in culture. These *in vitro* stimulated cells also showed suppressive function despite the fact that Ca^{2+} influx after treatment with thapsigargin or anti-CD3 plus Fab(2) fragment was absent (data not shown).

Discussion

The severe primary immunodeficiencies caused by defects in STIM1 or ORAI1 impressively illustrate the key role for SOCE in human lymphocyte function. While ORAI1 deficiency mainly manifests with severely increased susceptibility to infection (12, 25, 26), the immunological phenotype of STIM1 deficiency is more complex. Our description of a third kindred now allows the evaluation of 6 affected patients (9, 10) and reveals a consistent phenotype of a combined immunodeficiency that is less severe than in ORAI1 deficient patients and that is associated with important features of impaired immune regulation. These include early-onset autoimmune cytopenias in all 6 patients and lymphoproliferative disease, eczema, chronic diarrhea and arthritis in some of them (9, 10). Store-operated Ca^{2+} entry is required for activation, differentiation, and effector functions of most lymphocyte populations (27, 28). Impairment of antimicrobial effector lymphocytes could readily explain impaired infection control, but lymphoproliferation and autoimmunity are consequences of enhanced lymphocyte activation and therefore more difficult to explain. Since the defects also affect regulatory lymphocytes, this may imply that the consequences of STIM1 deficiency have greater impact on tolerogenic than on immunogenic effector functions. Our studies were therefore designed to more precisely define the impairment of antigen-specific effector and regulatory T cell immunity in human STIM1 deficiency.

The homozygous Arg429Cys STIM1 point mutation detected in the two reported siblings differs from the previously described E128RfsX9 frame shift (10) and 1538-1G>A splice site mutations (9) in that STIM1 protein expression was largely unaffected in our patients. Arg429 is located within a cytoplasmic STIM1 domain (alternatively named CRAC activation domain, CAD (29), STIM1 Orai activating region, SOAR (30), ORAI1-activating small fragment, OASF (31) or Coiled-coil fragment b9, CCb9 (32)) that binds directly to the N and C termini of ORAI1 and that is sufficient for CRAC channel opening (29). The mutation completely abolished Ca^{2+} influx in purified $CD3^+$ T cells and *in vitro* expanded regulatory T cells (data not shown) similar to the observations in EBV transformed B cell lines and fibroblasts of the previously reported STIM1 deficient patients (9, 10). Moreover, the clinical presentation including the dental enamel defect, anhidrosis, mild muscular hypotonia and non-reactive pupils as well as the onset and severity of immunodeficiency and immune dysregulation was comparable in all 6 STIM1 deficient patients (9, 10). Interestingly, the clinically asymptomatic heterozygous mother showed a partial impairment of Ca^{2+} flux, which is similar to the Arg91Trp mutation in ORAI1 (26), but not to other loss-of function mutations in that protein (25). It is tempting to speculate that the Arg429Cys mutation exerts a dominant negative effect on CRAC channel function by interfering either with the multimerization of STIM1 or the interaction of STIM1 with ORAI1. This will have to be clarified in future experiments.

A key feature of STIM1 deficiency is a broad susceptibility to viral infections that includes enterovirus and several herpesviruses such as EBV, CMV, VZV, HSV and HHV-8. However, antiviral immune responses have so far not been analyzed in humans or mice with CRAC channel deficiencies. Both of our patients had persistent EBV and CMV infection and suffered from recurrent HSV1 reactivation. This was not associated with a failure to mount virus-specific IgG antibody responses, which were detectable against all three viruses. This ability to mount at least some antigen-specific antibody responses is consistent with findings in STIM1 deficient bone marrow chimeric mice (33) and supports the notion that STIM1-dependent SOCE is dispensable for the differentiation of $CD4^+$ T cells into helper T cells and that of B cells into antibody secreting plasma cells *in vivo*. More unexpectedly, we could demonstrate significant antiviral $CD8^+$ T cell populations specific for CMV and to a lesser extent for EBV by MHC-peptide tetramer staining. Previous experiments on antigen-specific T cell responses in a mouse model of experimental autoimmune encephalitis yielded conflicting results on the requirement of STIM1 for the generation of neuroantigen-specific T cell responses *in vivo* (34, 35). The virus-specific T cells in P5 were reactive to antigen, since they could be further expanded by stimulation with their cognate peptide in vitro. The predominance of terminally differentiated $CD8^+$ T cells in the context of chronic viral infections further suggested that their cellular differentiation program was not dependent on STIM1. Overall, these data indicated that the priming phase of antiviral $CD8^+$ T cell responses was not dependent on STIM1.

Despite the presence of these important elements of antiviral immunity, the patients failed to control their infections. It is likely that one important factor was the reduced proliferative response of STIM1 deficient T cells (10, 17, 33), which could only partially be restored by the addition of IL-2. In the context of a viral infection, such a delay in the amplification of antiviral T cells is probably critical for virus control. Another relevant factor was the partial impairment of T cell effector functions. As expected from murine studies, the impairment in the production of cytokines was most obvious (17, 33–35). In particular, we observed a dramatic reduction in the ability of T cells to produce IL-2, IFN-γ and IL-17. In contrast, the production of IL-4 was largely retained. This may be explained by the fact that the Ca^{2+} dependent transcription factor NFAT, which is essential for cytokine production by T cells, also mediates a negative feedback loop that inhibits IL-4 transcription leading to a strong Th2 bias in NFAT1 deficient mice (36, 37). Expression of high levels of PD1 and 2B4, receptors associated with a poorly functional, “exhausted” CTL phenotype (19, 38) may also have contributed to the poor antiviral T cell activity.

In contrast to the severe impairment of cytokine production, the patient CTL showed normal antiviral cytotoxicity *in vitro*. This was unexpected, since we have recently demonstrated (16) and confirmed in this study that both ORAI1 and STIM1 deficient human NK cells have a severe cytotoxicity defect due to impaired lytic granule mobilization. The fact that NK cells were analyzed directly *ex vivo* or after short-term IL-2 stimulation, while CTL were analyzed after prolonged culture with PHA or viral peptide and IL-2 could explain these differences. However, different dependence of cytotoxicity on STIM1 in the two cell types remains another possibility. Overall, these data show that the effector phase of T cell responses is only partially affected by STIM1 deficiency. This conclusion is supported by the observation in mice, that STIM1 deficient $CD4^+$ T cells are capable of inducing acute graft versus host disease upon transfer into allogeneic recipients, albeit with delayed or reduced severity of disease, and with lower levels of inflammatory cytokines (33).

The other key clinical feature of STIM1 deficiency is impaired immune regulation, most consistently manifesting as autoimmune cytopenia and lymphoproliferation. Both of our patients and 3 of the 4 previously reported STIM1 deficient patients had splenomegaly and lymphoadenopathy. In addition, P5 developed EBV associated lymphoproliferation in the

lung, which was unusually severe and destructive. The excellent clinical response to rituximab treatment may indicate that the disease was at least in part driven by the EBV infection. However, lymphoid infiltrations in the absence of infection have also been observed in the lung, liver, spleen and lymph nodes of STIM1 deficient mice (33) and in mice lacking STIM1 and STIM2 exclusively in T cells (17). In the latter mice, the infiltrates showed a high proportion of myelomonocytic cells, while activated $CD8^+$ T cells predominated in our patient. Another relevant observation in this context is the moderate T cell lymphocytosis that was documented in 3 of the 6 STIM1 deficient patients. Again, viral infections could contribute, but lymphocytosis has also been observed in the mouse models in the absence of infection (17). T cell lymphoproliferative disease in an immunodeficiency associated with impaired T cell proliferation *in vitro* is counter-intuitive, but one potential explanation could be the increased proliferation of STIM1 deficient T cells towards homeostatic stimuli *in vivo* (33). Another possibility would be impaired apoptosis, but CD95 or anti-CD3 induced apoptosis was normal in our and one previously reported patient ((10) and data not shown).

Since Ca^{2+} flux and NFAT activation are crucial for Treg differentiation and function (17, 39, 40), a role for Treg cells in the phenotype of immune dysregulation in STIM1 deficiency has been postulated. In fact, the clinical phenotype of lymphoproliferation with autoimmune cytopenia, eczema and bowel inflammation is in part reminiscent of FOXP3 deficiency. In support of this notion, mice lacking STIM1 and STIM2 in T cells have reduced numbers of Treg cells and their myelo- and lymphoproliferative phenotype could be prevented by transfer of wildtype $CD4^+CD25^+$ Treg cells. Moreover, the numbers of circulating Treg cells were reduced in one of the previously published STIM1 deficient patients (10). By contrast, the numbers of circulating $FOXP3^+$ T cells was only slightly reduced in our patient and FOXP3 expressing cells were abundant in his lymph nodes and lung. The patients Treg cells did however show some important phenotypic differences compared to control Treg cells as their expression of CD25 and CD39 was significantly reduced. STIM1 deficient $CD4^+CD25^+$ T cells (defined as Treg cells) isolated from the patient showed good suppressive function in coincubation assays *in vitro*. These data are consistent with the observation of normal numbers and function of STIM1 deficient Treg cells in mice (17, 33). While our data show that STIM1 mediated SOCE in human Treg is not required for their suppressive function *in vitro*, this may not reflect the situation *in vivo*. In particular, Treg function *in vivo* is dependent on IL-2 (41-44), the secretion of which was severely impaired in our patient. Overall, the contribution of impaired Treg differentiation and function to the immune dysregulation in STIM1 deficiency remains incompletely defined.

In summary, this first comprehensive analysis of the immune system in a STIM1 deficient patient revealed that the complex clinical phenotype of human STIM1 deficiency cannot be easily explained by absent SOCE in T cells alone leading to impaired peripheral regulatory and effector T cell function. Intrinsic defects in other immune cell populations such as NK cells, NKT cells and B cells (45, 46) are likely to contribute to the observed phenotype of immunodeficiency and immune dysregulation.

Supplementary Material

Refer to Web version on PubMed Central for supplementary material.

Acknowledgments

We thank the patients' parents for their trust and all involved physicians and scientists for helpful discussion. Excellent technical assistance was provided by technicians of the CCI advanced diagnostic unit.

References

1. Feske S. Calcium signalling in lymphocyte activation and disease. Nat Rev Immunol. 2007; 7:690–702. [PubMed: 17703229]
2. Oh-hora M, Rao A. Calcium signaling in lymphocytes. Curr Opin Immunol. 2008; 20:250–258. [PubMed: 18515054]
3. Liou J, Kim ML, Heo WD, Jones JT, Myers JW, Ferrell JE Jr, Meyer T. STIM is a Ca2+ sensor essential for Ca2+-store-depletion-triggered Ca2+ influx. Curr Biol. 2005; 15:1235–1241. [PubMed: 16005298]
4. Roos J, DiGregorio PJ, Yeromin AV, Ohlsen K, Lioudyno M, Zhang S, Safrina O, Kozak JA, Wagner SL, Cahalan MD, Velicelebi G, Stauderman KA. STIM1, an essential and conserved component of store-operated Ca2+ channel function. J Cell Biol. 2005; 169:435–445. [PubMed: 15866891]
5. Prakriya M, Feske S, Gwack Y, Srikanth S, Rao A, Hogan PG. Orai1 is an essential pore subunit of the CRAC channel. Nature. 2006; 443:230–233. [PubMed: 16921383]
6. Vig M, Beck A, Billingsley JM, Lis A, Parvez S, Peinelt C, Koomoa DL, Soboloff J, Gill DL, Fleig A, Kinet JP, Penner R. CRACM1 multimers form the ion-selective pore of the CRAC channel. Curr Biol. 2006; 16:2073–2079. [PubMed: 16978865]
7. Yeromin AV, Zhang SL, Jiang W, Yu Y, Safrina O, Cahalan MD. Molecular identification of the CRAC channel by altered ion selectivity in a mutant of Orai. Nature. 2006; 443:226–229. [PubMed: 16921385]
8. Feske S, Picard C, Fischer A. Immunodeficiency due to mutations in ORAI1 and STIM1. Clin Immunol. 2010; 135:169–182. [PubMed: 20189884]
9. Byun M, Abhyankar A, Lelarge V, Plancoulaine S, Palanduz A, Telhan L, Boisson B, Picard C, Dewell S, Zhao C, Jouanguy E, Feske S, Abel L, Casanova JL. Whole-exome sequencing-based discovery of STIM1 deficiency in a child with fatal classic Kaposi sarcoma. J Exp Med. 2010; 207:2307–2312. [PubMed: 20876309]
10. Picard C, McCarl CA, Papolos A, Khalil S, Luthy K, Hivroz C, LeDeist F, Rieux-Laucat F, Rechavi G, Rao A, Fischer A, Feske S. STIM1 mutation associated with a syndrome of immunodeficiency and autoimmunity. N Engl J Med. 2009; 360:1971–1980. [PubMed: 19420366]
11. Schlesier M, Niemeyer C, Duffner U, Henschen M, Tanzi-Fetta R, Wolff-Vorbeck G, Drager R, Brandis M, Peter HH. Primary severe immunodeficiency due to impaired signal transduction in T cells. Immunodeficiency. 1993; 4:133–136. [PubMed: 8167687]
12. Feske S, Muller JM, Graf D, Kroczek RA, Drager R, Niemeyer C, Baeuerle PA, Peter HH, Schlesier M. Severe combined immunodeficiency due to defective binding of the nuclear factor of activated T cells in T lymphocytes of two male siblings. Eur J Immunol. 1996; 26:2119–2126. [PubMed: 8814256]
13. Le Deist F, Hivroz C, Partiseti M, Thomas C, Buc HA, Oleastro M, Belohradsky B, Choquet D, Fischer A. A primary T-cell immunodeficiency associated with defective transmembrane calcium influx. Blood. 1995; 85:1053–1062. [PubMed: 7531512]
14. Partiseti M, Le Deist F, Hivroz C, Fischer A, Korn H, Choquet D. The calcium current activated by T cell receptor and store depletion in human lymphocytes is absent in a primary immunodeficiency. J Biol Chem. 1994; 269:32327–32335. [PubMed: 7798233]
15. Feske S, Draeger R, Peter HH, Eichmann K, Rao A. The duration of nuclear residence of NFAT determines the pattern of cytokine expression in human SCID T cells. J Immunol. 2000; 165:297–305. [PubMed: 10861065]
16. Maul-Pavicic A, Chiang SC, Rensing-Ehl A, Jessen B, Fauriat C, Wood SM, Sjoqvist S, Hufnagel M, Schulze I, Bass T, Schamel WW, Fuchs S, Pircher H, McCarl CA, Mikoshiba K, Schwarz K, Feske S, Bryceson YT, Ehl S. ORAI1-mediated calcium influx is required for human cytotoxic lymphocyte degranulation and target cell lysis. Proc Natl Acad Sci U S A. 2011
17. Oh-Hora M, Yamashita M, Hogan PG, Sharma S, Lamperti E, Chung W, Prakriya M, Feske S, Rao A. Dual functions for the endoplasmic reticulum calcium sensors STIM1 and STIM2 in T cell activation and tolerance. Nat Immunol. 2008; 9:432–443. [PubMed: 18327260]

18. Rensing-Ehl A, Warnatz K, Fuchs S, Schlesier M, Salzer U, Draeger R, Bondzio I, Joos Y, Janda A, Gomes M, Abinun M, Hambleton S, Cant A, Shackley F, Flood T, Waruiru C, Beutel K, Siepermann K, Dueckers G, Niehues T, Wiesel T, Schuster V, Seidel MG, Minkov M, Sirkia K, Kopp MV, Korhonen M, Schwarz K, Ehl S, Speckmann C. Clinical and immunological overlap between autoimmune lymphoproliferative syndrome and common variable immunodeficiency. Clin Immunol. 2010; 137:357–365. [PubMed: 20832369]

19. Bengsch B, Seigel B, Ruhl M, Timm J, Kuntz M, Blum HE, Pircher H, Thimme R. Coexpression of PD-1, 2B4, CD160 and KLRG1 on exhausted HCV-specific CD8+ T cells is linked to antigen recognition and T cell differentiation. PLoS Pathog. 2010; 6:e1000947. [PubMed: 20548953]

20. Appay V, van Lier RA, Sallusto F, Roederer M. Phenotype and function of human T lymphocyte subsets: consensus and issues. Cytometry A. 2008; 73:975–983. [PubMed: 18785267]

21. Khan N, Hislop A, Gudgeon N, Cobbold M, Khanna R, Nayak L, Rickinson AB, Moss PA. Herpesvirus-specific CD8 T cell immunity in old age: cytomegalovirus impairs the response to a coresident EBV infection. J Immunol. 2004; 173:7481–7489. [PubMed: 15585874]

22. Diana J, Lehuen A. NKT cells: friend or foe during viral infections? Eur J Immunol. 2009; 39:3283–3291. [PubMed: 19830742]

23. Lanier LL. Evolutionary struggles between NK cells and viruses. Nat Rev Immunol. 2008; 8:259–268. [PubMed: 18340344]

24. Mandapathil M, Lang S, Gorelik E, Whiteside TL. Isolation of functional human regulatory T cells (Treg) from the peripheral blood based on the CD39 expression. J Immunol Methods. 2009; 346:55–63. [PubMed: 19450601]

25. McCarl CA, Picard C, Khalil S, Kawasaki T, Rother J, Papolos A, Kutok J, Hivroz C, Ledeist F, Plogmann K, Ehl S, Notheis G, Albert MH, Belohradsky BH, Kirschner J, Rao A, Fischer A, Feske S. ORAI1 deficiency and lack of store-operated Ca2+ entry cause immunodeficiency, myopathy, and ectodermal dysplasia. J Allergy Clin Immunol. 2009; 124:1311–1318. e1317. [PubMed: 20004786]

26. Feske S, Gwack Y, Prakriya M, Srikanth S, Puppel SH, Tanasa B, Hogan PG, Lewis RS, Daly M, Rao A. A mutation in Orai1 causes immune deficiency by abrogating CRAC channel function. Nature. 2006; 441:179–185. [PubMed: 16582901]

27. Feske S. ORAI1 and STIM1 deficiency in human and mice: roles of store-operated Ca2+ entry in the immune system and beyond. Immunol Rev. 2009; 231:189–209. [PubMed: 19754898]

28. Oh-hora M. Calcium signaling in the development and function of T-lineage cells. Immunol Rev. 2009; 231:210–224. [PubMed: 19754899]

29. Park CY, Hoover PJ, Mullins FM, Bachhawat P, Covington ED, Raunser S, Walz T, Garcia KC, Dolmetsch RE, Lewis RS. STIM1 clusters and activates CRAC channels via direct binding of a cytosolic domain to Orai1. Cell. 2009; 136:876–890. [PubMed: 19249086]

30. Yuan JP, Zeng W, Dorwart MR, Choi YJ, Worley PF, Muallem S. SOAR and the polybasic STIM1 domains gate and regulate Orai channels. Nat Cell Biol. 2009; 11:337–343. [PubMed: 19182790]

31. Muik M, Fahrner M, Derler I, Schindl R, Bergsmann J, Frischauf I, Groschner K, Romanin C. A Cytosolic Homomerization and a Modulatory Domain within STIM1 C Terminus Determine Coupling to ORAI1 Channels. J Biol Chem. 2009; 284:8421–8426. [PubMed: 19189966]

32. Kawasaki T, Lange I, Feske S. A minimal regulatory domain in the C terminus of STIM1 binds to and activates ORAI1 CRAC channels. Biochem Biophys Res Commun. 2009; 385:49–54. [PubMed: 19433061]

33. Beyersdorf N, Braun A, Vogtle T, Varga-Szabo D, Galdos RR, Kissler S, Kerkau T, Nieswandt B. STIM1-independent T cell development and effector function in vivo. J Immunol. 2009; 182:3390–3397. [PubMed: 19265116]

34. Ma J, McCarl CA, Khalil S, Luthy K, Feske S. T-cell-specific deletion of STIM1 and STIM2 protects mice from EAE by impairing the effector functions of Th1 and Th17 cells. Eur J Immunol. 2010

35. Schuhmann MK, Stegner D, Berna-Erro A, Bittner S, Braun A, Kleinschnitz C, Stoll G, Wiendl H, Meuth SG, Nieswandt B. Stromal interaction molecules 1 and 2 are key regulators of autoreactive

T cell activation in murine autoimmune central nervous system inflammation. J Immunol. 2010; 184:1536–1542. [PubMed: 20028655]

36. Kiani A, Viola JP, Lichtman AH, Rao A. Down-regulation of IL-4 gene transcription and control of Th2 cell differentiation by a mechanism involving NFAT1. Immunity. 1997; 7:849–860. [PubMed: 9430230]
37. Ranger AM, Oukka M, Rengarajan J, Glimcher LH. Inhibitory function of two NFAT family members in lymphoid homeostasis and Th2 development. Immunity. 1998; 9:627–635. [PubMed: 9846484]
38. Blackburn SD, Shin H, Haining WN, Zou T, Workman CJ, Polley A, Betts MR, Freeman GJ, Vignali DA, Wherry EJ. Coregulation of CD8+ T cell exhaustion by multiple inhibitory receptors during chronic viral infection. Nat Immunol. 2009; 10:29–37. [PubMed: 19043418]
39. Tone Y, Furuuchi K, Kojima Y, Tykocinski ML, Greene MI, Tone M. Smad3 and NFAT cooperate to induce Foxp3 expression through its enhancer. Nat Immunol. 2008; 9:194–202. [PubMed: 18157133]
40. Wu Y, Borde M, Heissmeyer V, Feuerer M, Lapan AD, Stroud JC, Bates DL, Guo L, Han A, Ziegler SF, Mathis D, Benoist C, Chen L, Rao A. FOXP3 controls regulatory T cell function through cooperation with NFAT. Cell. 2006; 126:375–387. [PubMed: 16873067]
41. Furtado GC, Curotto de Lafaille MA, Kutchukhidze N, Lafaille JJ. Interleukin 2 signaling is required for CD4(+) regulatory T cell function. J Exp Med. 2002; 196:851–857. [PubMed: 12235217]
42. Setoguchi R, Hori S, Takahashi T, Sakaguchi S. Homeostatic maintenance of natural Foxp3(+) CD25(+) CD4(+) regulatory T cells by interleukin (IL)-2 and induction of autoimmune disease by IL-2 neutralization. J Exp Med. 2005; 201:723–735. [PubMed: 15753206]
43. Thornton AM, Donovan EE, Piccirillo CA, Shevach EM. Cutting edge: IL-2 is critically required for the in vitro activation of CD4+CD25+ T cell suppressor function. J Immunol. 2004; 172:6519–6523. [PubMed: 15153463]
44. Thornton AM, Piccirillo CA, Shevach EM. Activation requirements for the induction of CD4+CD25+ T cell suppressor function. Eur J Immunol. 2004; 34:366–376. [PubMed: 14768041]
45. Limnander A, Depeille P, Freedman TS, Liou J, Leitges M, Kurosaki T, Roose JP, Weiss A. STIM1, PKC-delta and RasGRP set a threshold for proapoptotic Erk signaling during B cell development. Nat Immunol. 2011; 12:425–433. [PubMed: 21441934]
46. Matsumoto M, Fujii Y, Baba A, Hikida M, Kurosaki T, Baba Y. The Calcium Sensors STIM1 and STIM2 Control B Cell Regulatory Function through Interleukin-10 Production. Immunity. 2011; 34:703–714. [PubMed: 21530328]
47. van den Beemd R, Boor PP, van Lochem EG, Hop WC, Langerak AW, Wolvers-Tettero IL, Hooijkaas H, van Dongen JJ. Flow cytometric analysis of the Vbeta repertoire in healthy controls. Cytometry. 2000; 40:336–345. [PubMed: 10918284]

A

	Patient 1*	Patient 2*	Patient 3*	Patient 4†	Patient 5	Patient 6
Mutation	E136X	NA	E136X	1538-1 G>A	R429C	R429C
Infections						
Viral	CMV, VZV	EBV, enterovirus	NA	HHV-8	CMV, EBV, HSV	CMV, EBV, HSV
Bacterial	Pneumonia, otitis, sepsis	NA	Sepsis	NA	Pneumonia, otitis, sepsis	Pneumonia, sepsis
Immune dysregulation						
Cytopenia (onset)	AIHA, ITP	AIHA, ITP	ITP	AIHA	AIHA, ITP (2 mo)	AIHA, ITP
Eczema	NA	NA	NA	Yes, mild	Yes, severe (1y)	Yes, severe
Lymphoproliferation	Spleen, liver, LN	Spleen, liver, LN	None	Spleen, liver	Spleen, LN	Liver
Other					Chronic diarrhea (5y)	
Other						
Enamel defect	Yes	Yes	Yes	NA	Yes	Yes
Anhydrosis	NA	NA	NA	NA	Yes	Yes
Mydriasis	Yes	Yes	Yes	NA	Yes	Yes
Muscular hypotonia	Yes	Yes	Yes	NA	Yes, mild	Yes, mild
Cell counts (age)					**5y**	**14mo**
Lymphocytes, µl	2200	7000	3900	§	6150	9152.00
CD3, µl	1826	3850	2457	§	5794	6309.00
CD4, µl	1056	3150	1950	§	3463	4234.00
CD8, µl	638	560	351	§	2272	1488.00
CD45RA+ of CD4+	50%	NA	NA	NA	3,4%	NA
NK cells, µl	NA	NA	468	§	137	890.00
B cells, µl	176	2590	819	§	69	1471.00
Immunoglobulins					**5y**	**14 mo**
IgG, g/l	17,0	0,42	3.36	§	7,1	13,4
IgM, g/l	0,82	0,23	0,44	§	0,9	0,69
IgA, g/l	0,71	0,7	0,11	§	1,09	0,52
IgE, kU/l	NA	NA	NA	§	7,42	3,12
Specific antibodies						
After vaccination	NA	NA	NA	NA	Tet+, Rub+, HiB-, PN- MM-	HiB-
After infection	NA	NA	NA	NA	EBV+, CMV+, HSV+	CMV+, HSV+
Reported Outcome	Died 9 y (during HSCT)	Died 1,5 y (encephalitis)	Alive (HSCT 1,2 y)	Died 2 y (Kaposi)	Alive (HSCT 6 y)	Died 1,7 y (sepsis)

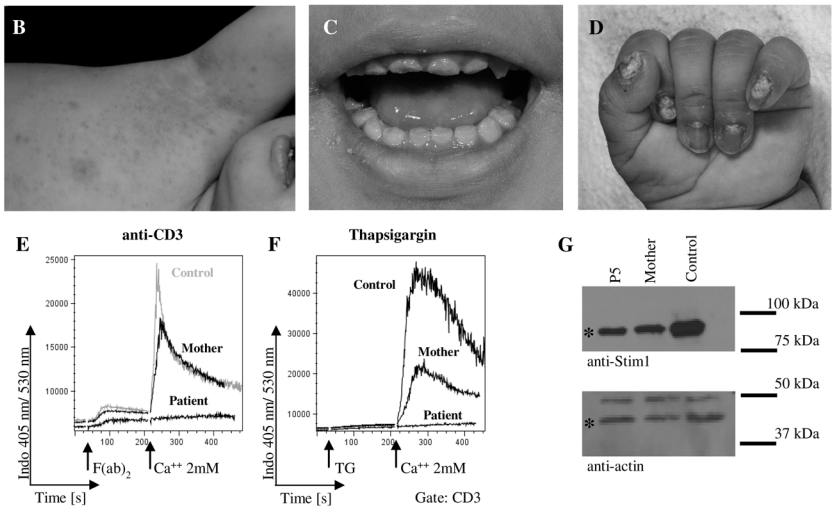

Figure 1. Clinical presentation of two new patients with STIM1 deficiency

A, Clinical presentation and basic immunological data of the two patients described in this report (P5 and P6) in comparison to data from the four previously published patients. AIHA = autoimmune haemolytic anemia, ITP = idiopathic thrombocytopenic purpura, n.a. = information not available, tet = tetanus, rub = rubella, HiB = hemophilus influenzae type B, PN = pneumococcus, MM = measles and mumps, HSCT = hematopoetic stem cell transplantation. *B*, Eczematous skin lesions of P5. (C) Dental enamel defect of P5. *D*, Nail dysplasia of P6. *E and F*, Calcium flux in MACS purified T cells from P5, the heterozygous mother and a healthy control in response to stimulation with anti-CD3 (5 µg/ml) and $F(ab)_2$ fragment (E) or thapsigargin (F). The results were obtained in two independent experiments, collecting approximately 600 events per second during FACS analysis. The measurement was started in Ca^{2+}-free medium and calcium was added at the indicated time point. *G*,

Western blot analysis of lysates from EBV LCL of P5, the heterozygous mother and a healthy donor incubated with anti-STIM1 (upper panel) and anti-actin antibodies as a loading control (lower panel). Specific bands are designated by an asterisk. Representative blot from 3 independent experiments. *(10), †(9)

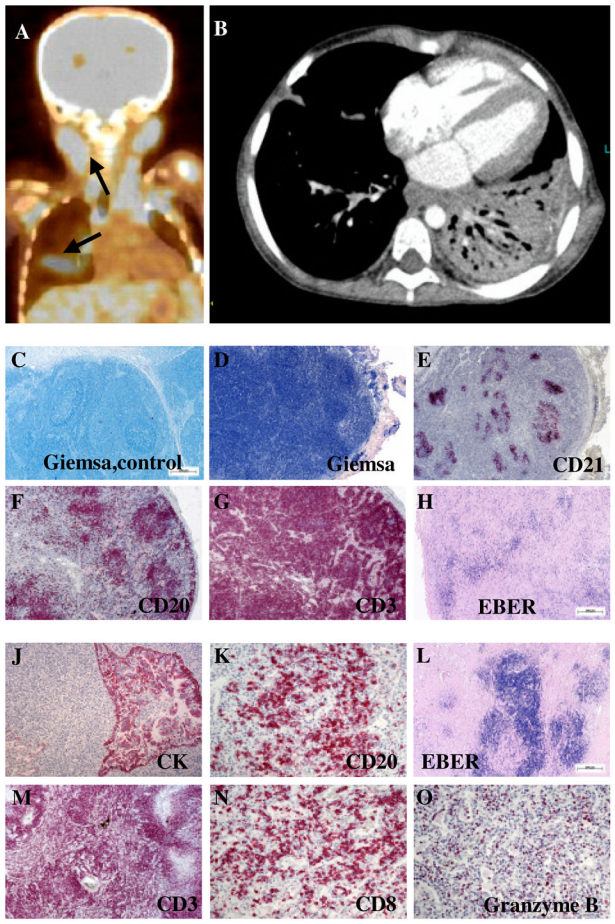

Figure 2. Destructive EBV positive lymphoproliferative disease

A, Positron emission tomography (PET) scan of P5. Arrows indicate areas of high metabolic activity reflecting lymphoproliferative disease. *B*, Pulmonary CT scan of P5 showing a dense infiltrate of the left lower lobe. *C-H*, Lymph node histology: Giemsa staining of a tumor-free lymph node from a control patient with cancer (*C*) and the lymph node from P5 (*D*). Immunohistological staining of follicular dendritic cells (anti-CD21; E), B cells (anti-CD20; F) and T cells (anti-CD3; G). The anti-EBER (*H*) staining shows the presence of EBV infected cells. *J-O*, Lung histology: Immunohistological staining of cytokeratin (*J*), B cells (anti-CD20; *K*) and T cells (anti-CD3; *M*), that were predominantly CTL (anti-CD8; *N*) expressing high amounts of Granzyme B (O). The lung lesions were also highly positive for EBV infected cells (anti-EBER; *L*). The magnification was 2,5x (C-F,H and L), 5x (G,J and M) and 20x (K,N and O).

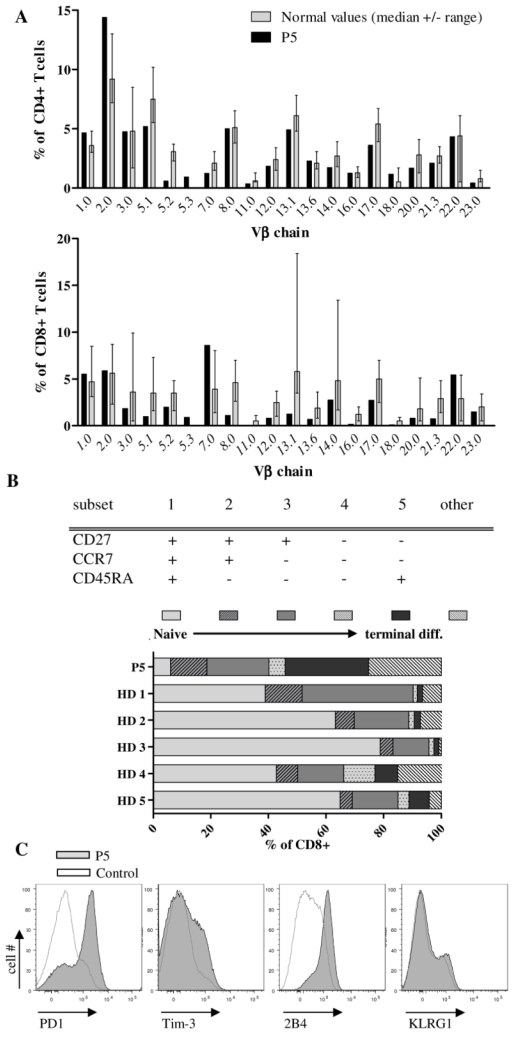

Figure 3. T cell repertoire and phenotype

A, Percentage of $CD4^+$ (upper panel) and $CD8^+$ (lower panel) T cells expressing the indicated Vβ chains as determined by flow cytometry. The grey columns and error bars indicate the median and range of healthy controls (47). *B*, Differentiation subsets of $CD8^+$ T cells according to their expression of CD45RA, CCR7 and CD27 (upper panel). Percentage of $CD8^+$ T cells in the respective subset in the patient and 5 healthy donors (lower panel). Representative results from three measurements during hospitalization of P5. *C*, Expression of PD-1, Tim-3, 2B4 and KLRG1 on $CD8^+$ T cells from the patient (tinted grey) and a representative healthy adult (grey line).

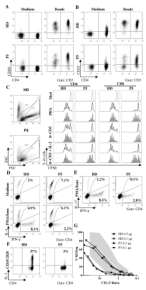

Figure 4. Partial impairment of T cell activation and T cell effector functions

A, B, Expression of CD69 (*A*) and CD25 (*B*) on $CD4^+$ and $CD8^+$ T cells after 24h incubation of PBMC in medium alone or supplemented with anti-CD3/CD28 beads. Dot plots are gated on $CD3^+$ T cells. Results are representative of two independent experiments. *C*, CFSE proliferation assay using PBMC from the patient and a healthy donor after stimulation with PHA, anti-CD3 or anti-CD3 + IL-2 for 6 days. The histograms are gated on $CD3^+CD4^+$ T cells (left panels) or $CD3^+CD8^+$ T cells (right panels). All lymphocytes (line) including blasted T cells and T cell blasts with a high forward/side scatter profile (shaded grey)were analyzed separately. Three independent experiments were carried out. *D, E*, Cytokine production of $CD4^+$ T cells after stimulation of PBMC with PMA and Ionomycin for 4 hours in the presence of Brefeldin A. Representative results for two measurements. *F*, IL-2 production of $CD4^+$ T cells after stimulation of PBMC with anti-CD3/antiCD-28 beads for 16h in the presence of Brefeldin A. Results obtained from two experiments. *G*, Cytotoxicity of PHA/IL-2 T cell blasts against ^{51}Cr labelled L1210 target cells loaded with different concentrations of anti-CD3. Two different experiments showed similar results.

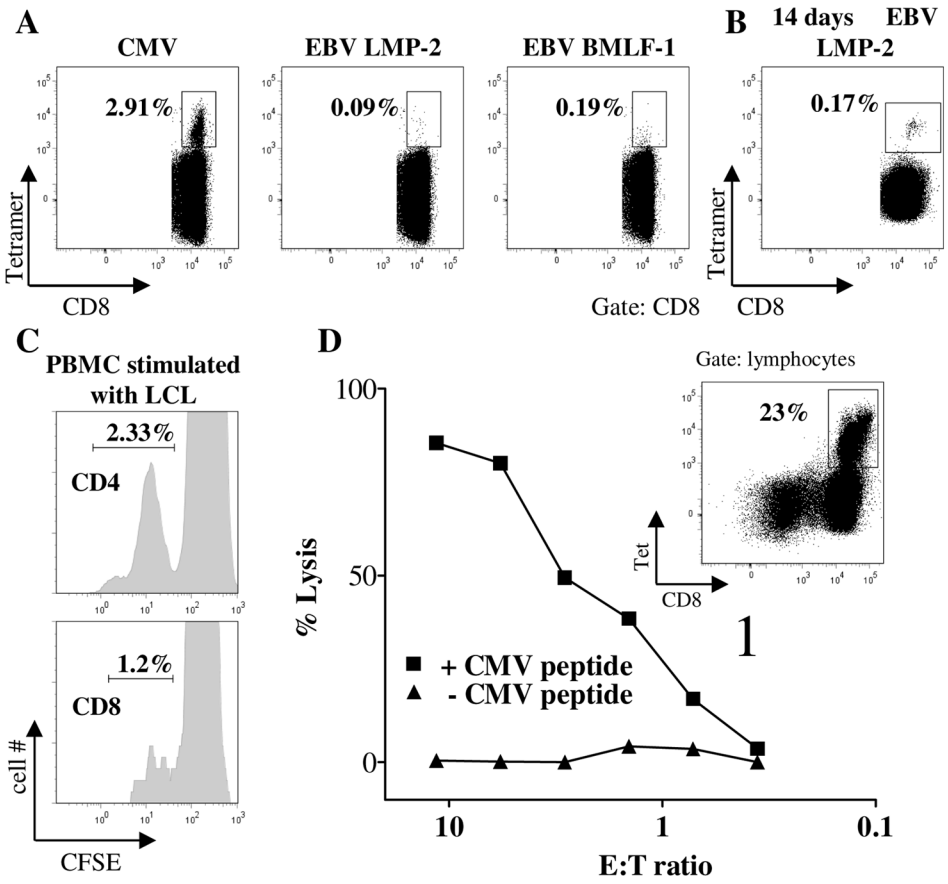

Figure 5. Antiviral T cells are generated and respond to antigen stimulation *in vitro*

A, Frequency of $CD8^+$ T cells binding HLA-A2 tetramers labelled with epitopes of CMV (pp65) and EBV (LMP-2 and BMLF-1). *B*, Staining of $CD8^+$ T cells with LMP-2 tetramer after 14 days culture of PBMC from the patient with autologous irradiated PBMC pulsed with LMP-2 peptide. *C*, CFSE dilution of $CD4^+$ (upper panel) and $CD8^+$ T cells (lower panel) incubated with autologous EBV-LCL for 3 days. *D*, PBMC were cultured with CMV pp65 peptide for 3 weeks leading to an expansion of virus-specific CTL (insert indicates the fraction of $CD8^+$ T cells expressing a pp65 specific TCR as detected by tetramer staining). Lytic activity of these cells was tested on autologous ^{51}Cr loaded EBV-LCL target cells that were used unpulsed (triangles) or after incubation with CMV p65 peptide (squares). Spontaneous lysis was below 30%.

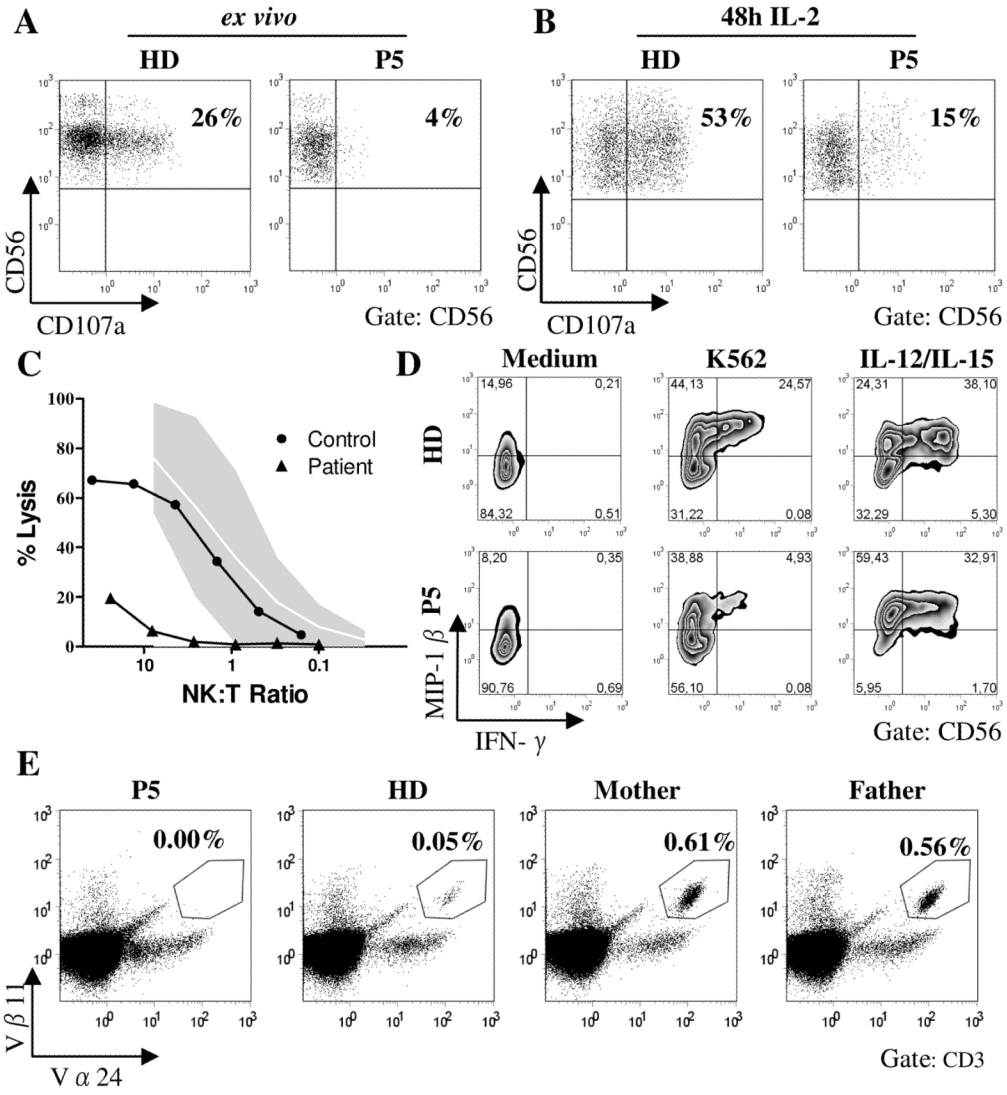

Figure 6. Impaired NK cell function and absent NKT cells

A,*B*, Degranulation of resting (*A*) and IL-2 activated (*B*) NK cells after stimulation of PBMC with K562 target cells as assessed by anti-CD107a expression. Dot plots are gated on $CD3^{-}CD56^{+}$ lymphocytes. Representative results from two experiments. *C*, Lytic activity of MACS purified NK cells on ^{51}Cr labelled K562 target cells. The gray area represents the normal range of lytic activity using NK cells from healthy donors. *D*, MACS purified NK cells were either incubated in medium alone (left panel), stimulated with K562 target cells (middle panel) or with IL-12 and IL-15 (right panel) for 5h and analyzed for intracellular expression of IFN-γ and MIP-1β. Representative results from two independent experiments. *E*, Frequency of NKT cells among $CD3^{+}$ T cells as determined by staining with anti-Vβ11 and Vα24 antibodies. Dot plots are gated on $CD3^{+}$ lymphocytes. Measurement was repeated once with similar results. Normal values (n=59) in our lab range from 0,008 to 0,76% of $CD3^{+}$ T cells with a median of 0,045%. The 5^{th} percentile was 0,008% and the 95^{th} percentile 0,56%.

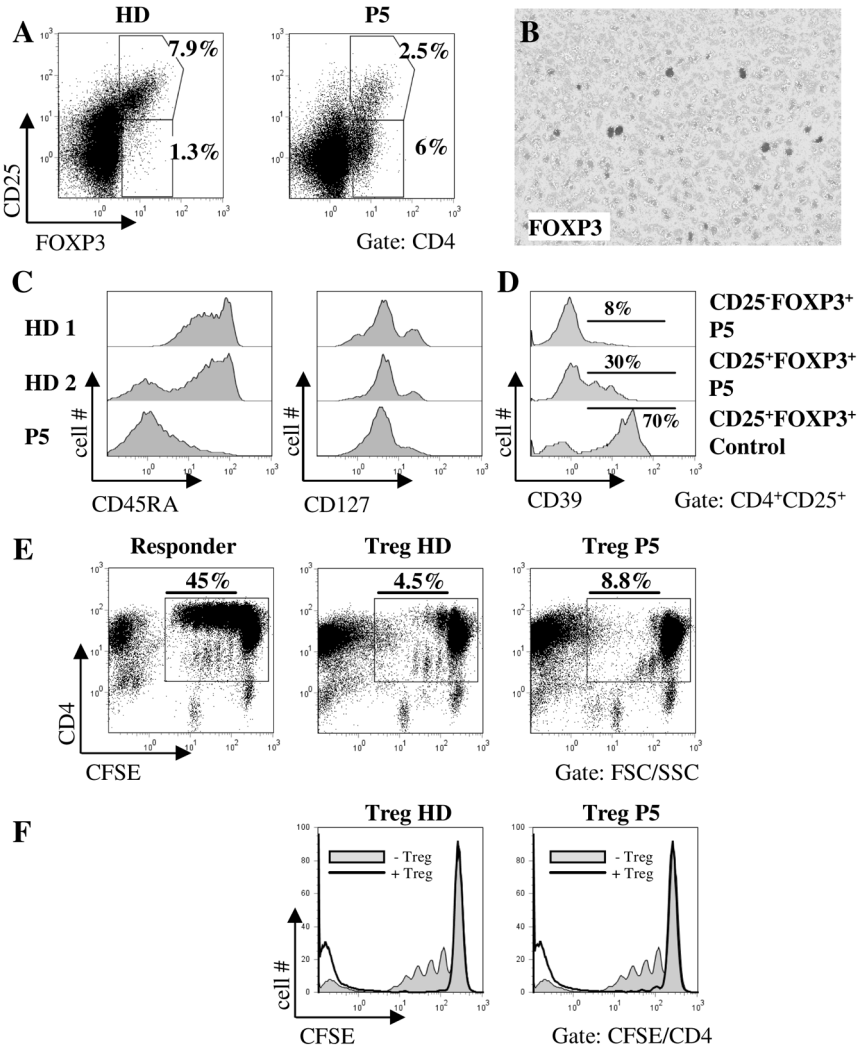

Figure 7. Phenotype and function of $CD25^+FOXP3^+$ regulatory T cells

A, PBMC from the patient and a healthy donor were stained for CD3, CD4, CD25 and FOXP3. Dot plots are gated on $CD3^+CD4^+$ lymphocytes. Results are representative of 2 independent experiments. *B*, Immunohistological analysis of the pulmonary lymphoproliferative lesion using antibodies to FOXP3 (dark grey). *C*, Expression of CD45RA (left) and CD127 (right) on $CD4^+CD25^+$ MACS purified T cells. *D*, Expression of CD39 on Treg cells. Histograms are gated on $CD3^+CD4^+CD25^+FOXP3^+$ or FOXP3− lymphocytes as indicated. *E*, MACS isolated $CD4^+CD25^-$responder T cells from a healthy donor were labelled with CFSE and stimulated with irradiated allogeneic PBMC and anti-CD3 in the absence (left panel) or presence of $CD4^+CD25^{hi}$ Treg from the same donor (middle panel) or the patient (right panel). Dot plots are gated on lymphocytes defined by forward and side scatter and are representative of 2 independent experiments. *F*, Histogram overlays of the same data illustrating the suppressive effect of control (left panel) and patient (right panel) Treg cells.